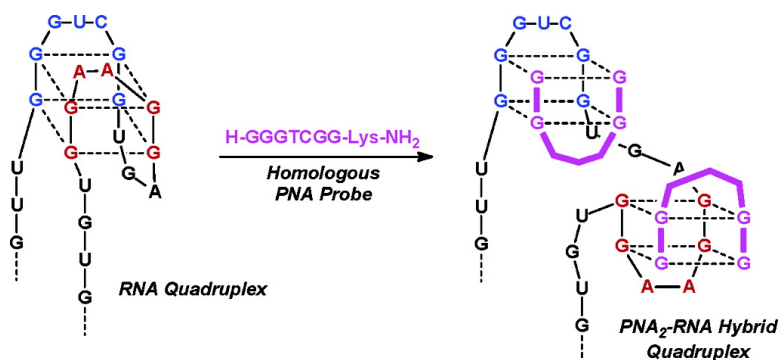


## RNA Guanine Quadruplex Invasion by Complementary and Homologous PNA Probes

Violeta L. Marin, and Bruce A. Armitage

*J. Am. Chem. Soc.*, **2005**, 127 (22), 8032-8033 • DOI: 10.1021/ja051102y • Publication Date (Web): 14 May 2005

Downloaded from <http://pubs.acs.org> on March 25, 2009



### More About This Article

Additional resources and features associated with this article are available within the HTML version:

- Supporting Information
- Links to the 4 articles that cite this article, as of the time of this article download
- Access to high resolution figures
- Links to articles and content related to this article
- Copyright permission to reproduce figures and/or text from this article

[View the Full Text HTML](#)





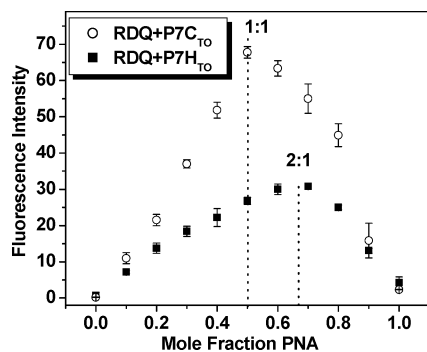


**Figure 2.** Job plot for complementary and homologous PNAs binding to **RDQ** at a total concentration of  $0.5 \mu\text{M}$  monitored by fluorescence. Samples were prepared in 10 mM Tris/HCl (pH = 7.0) with 100 mM KCl and were annealed prior to recording the spectra ( $\lambda_{\text{Ex}} = 495 \text{ nm}$ ).

CD spectroscopy is commonly used to detect hybridization reactions, but very little difference was observed in the spectra recorded for **RDQ** in the absence and presence of **P7C** (data not shown). This is due to the fact that the CD spectrum of **RDQ** is very similar to the CD spectrum previously reported for a PNA–RNA duplex.<sup>6</sup> Further support for successful hybridization of **P7C** was obtained from fluorescence experiments using a PNA probe end-labeled with a thiazole orange (TO) derivative. TO is essentially nonfluorescent in fluid solution but becomes strongly fluorescent when placed in a rigid environment.<sup>14</sup> Svanvik, Kubista, and co-workers demonstrated that TO–PNA conjugates exhibit enhanced fluorescence upon hybridization to complementary DNA strands, most likely due either to end-stacking of the fluorophore onto the PNA–DNA duplex or to partial intercalation into DNA nucleobases extending beyond the hybrid region.<sup>15</sup> Figure S2 illustrates fluorescence spectra recorded for **P7C**<sub>TO</sub> in solution and in the presence of **RDQ**. The fluorescence increases approximately 40-fold upon hybridization to the RNA. This was used to determine an equilibrium binding constant for PNA hybridization of  $8.1 \times 10^8 \text{ M}^{-1}$  (Figure S3).

We next synthesized PNA probe **P7H** to test for hybrid PNA–RNA quadruplex formation. This PNA is homologous to the same target site as the complementary probe **P7C**. The melting curve recorded for a 1:1 mixture of the homologous PNA and **RDQ** is shown in Figure 1 (triangles). In contrast to the complementary probe, a hypochromic transition is still observed in the presence of **P7H**. However, this transition occurs at much higher temperature ( $\Delta T_m = \text{ca. } 30 \text{ }^\circ\text{C}$ ), and the transition assigned to melting of the RNA duplex region is not observed. Substituting LiCl for KCl in the solution causes the  $T_m$  to decrease by approximately  $30 \text{ }^\circ\text{C}$ , and the hyperchromic transition due to melting of the RNA stem reappears (Figure S4). These results indicate that the **P7H** forms a hybrid quadruplex with **RDQ**.

A TO-labeled version of **P7H** demonstrated a 5-fold fluorescence enhancement in the presence of **RDQ** (Figure S5). Given the polymorphic nature of G-quadruplex structures in DNA, it was not immediately obvious how many PNA strands would hybridize to the intramolecular G-quadruplex in **RDQ**. Figure 2 shows that the complementary PNA forms a 1:1 hybrid, as expected based on the constraints of Watson–Crick base pairing. However, the homologous PNA clearly forms a 2:1 complex, meaning two **P7H**<sub>TO</sub> strands bind to a single **RDQ**. It is important to note that while **P7H** is perfectly homologous to the 7 nucleotide target site shown in Chart 1, hybridization should be mediated by the guanine bases that

participate in G-tetrad formation while the central non-G bases are less important. Thus, **P7H** is “G-homologous” to **RDQ** in several ways, depending on which two G-tracts it uses to form the hybrid quadruplex. For example, if one **P7H** hybridizes to the blue target region in Chart 1 (i.e., G<sub>1</sub>–G<sub>2</sub> and G<sub>3</sub>–G<sub>4</sub>), then the two G-tracts displaced from the **RDQ** quadruplex (i.e., G<sub>5</sub>–G<sub>6</sub> and G<sub>7</sub>–G<sub>8</sub>, shown in red in Chart 1) would be available for hybridizing with a second homologous PNA, with the only mismatches arising from the linkers joining the two G-tracts in the probe and target. The implications of this degeneracy on the sequence selectivity of homologous hybridization will be the subject of a future investigation.

These relatively short PNA probes overcome kinetic and thermodynamic obstacles to hybridization presented by the folded secondary structure of **RDQ**. Hybridization occurs within 10 min at room temperature and submicromolar PNA and RNA concentrations. The thermodynamic driving force for quadruplex invasion remains to be determined, although both duplex and quadruplex hybrids should involve more hydrogen bonding and  $\pi$ -stacking interactions than are present in the RNA quadruplex. Electrostatic interactions are likely favorable, as well, since hybridization will result in Coulombic attraction between the cationic PNA and the RNA target, while also relieving intrastrand electrostatic repulsions due to opening of the RNA quadruplex.

In conclusion, both complementary and homologous PNA probes invade an intramolecular RNA quadruplex and form stable PNA–RNA duplex and quadruplex structures, respectively.

**Acknowledgment.** We thank the National Institutes of Health (RO1 GM58547) and Carnegie Mellon University for financial support of this research, Dr. Babu Rao Renikuntla for synthesis of the thiazole orange derivative, and Laurel Grotzinger for expert technical assistance. V.M. thanks the CMU Department of Chemistry for a Harrison Legacy Dissertation Fellowship. MALDI-TOF mass spectra were recorded in the Center for Molecular Analysis at Carnegie Mellon University, supported by NSF Grants CHE-9808188 and DBI-9729351.

**Supporting Information Available:** UV melting curves, fluorescence spectra, and binding constant determination. This material is available free of charge via the Internet at <http://pubs.acs.org>.

## References

- (1) Davis, J. T. *Angew. Chem., Int. Ed.* **2004**, *43*, 668–698.
- (2) Simonsson, T. *Biol. Chem.* **2001**, *382*, 621–628.
- (3) Siddiqui-Jain, A.; Grand, C. L.; Bearss, D. J.; Hurley, L. H. *Proc. Natl. Acad. Sci. U.S.A.* **2002**, *99*, 11593–11598.
- (4) Gomez, D.; Lemarteleur, T.; Lacroix, L.; Mailliet, P.; Mergny, J.-L.; Riou, J. F. *Nucleic Acids Res.* **2004**, *32*, 371–379.
- (5) Nielsen, P. E.; Egholm, M.; Berg, R. H.; Buchardt, O. *Science* **1991**, *254*, 1498–1500.
- (6) Egholm, M.; Buchardt, O.; Christensen, L.; Behrens, C.; Freier, S. M.; Driver, D. A.; Berg, R. H.; Kim, S. K.; Norden, B.; Nielsen, P. E. *Nature* **1993**, *265*, 566–568.
- (7) Datta, B.; Armitage, B. A. *J. Am. Chem. Soc.* **2001**, *123*, 9612–9619.
- (8) Green, J. J.; Ying, L.; Klenerman, D.; Balasubramanian, S. *J. Am. Chem. Soc.* **2003**, *125*, 3763–3767.
- (9) Datta, B.; Schmitt, C.; Armitage, B. A. *J. Am. Chem. Soc.* **2003**, *125*, 4111–4118.
- (10) Darnell, J. C.; Jensen, K. B.; Jin, P.; Brown, V.; Warren, S. T.; Darnell, R. B. *Cell* **2001**, *107*, 489–499.
- (11) Ramos, A.; Hollingworth, D.; Pastore, A. *RNA* **2003**, *9*, 1198–1207.
- (12) Mergny, J.-L.; Phan, A.-T.; Lacroix, L. *FEBS Lett.* **1998**, *435*, 74–78.
- (13) Williamson, J. R. *Annu. Rev. Biophys. Biomol. Struct.* **1994**, *23*, 703–730.
- (14) Lee, L. G.; Chen, C.; Liu, L. A. *Cytometry* **1986**, *7*, 508–517.
- (15) Svanvik, N.; Westman, G.; Wang, D.; Kubista, M. *Anal. Biochem.* **2000**, *281*, 26–35.

JA051102Y